
Kinetics of the Autoxidation of a Jet-A Fuel

James M. Pickard

Kinetica, Inc., Mound Advanced Technology Center,
720 Mound Avenue, P.O. Box 182, Miamisburg, Ohio 45343-0182

E. Grant Jones

Innovative Scientific Solutions, Inc., 3845 Woodhurst Court,
Beavercreek, Ohio 45430-1658

ENERGY & FUELS[®]
AN AMERICAN CHEMICAL SOCIETY JOURNAL

Reprinted from
Volume 10, Number 5, Pages 1074-1077

Kinetics of the Autoxidation of a Jet-A Fuel

James M. Pickard*

Kinetica, Inc., Mound Advanced Technology Center, 720 Mound Avenue, P.O. Box 182,
Miamisburg, Ohio 45343-0182

E. Grant Jones

Innovative Scientific Solutions, Inc., 3845 Woodhurst Court, Beavercreek, Ohio 45430-1658

Received February 27, 1996. Revised Manuscript Received June 10, 1996[®]

Kinetics of the autoxidation of a Jet-A fuel (POSF-2827) were examined with a near-isothermal flowing test rig (NIFTR) using passivated heat-exchanger tubing over the range 438–478 K. Analysis of the O₂ dependence for autoxidation of fuel having an initial O₂ saturation of 2.5–100% resulted in a reaction order of 0.5. Analysis for air-saturated fuel data based on the expected chain mechanism for a half-order O₂ dependence and second-order termination yielded $\log(k_{\text{ap}}/M^{-1/2} \text{ s}^{-1}) = (12.9 \pm 0.4) - (36.9 \pm 0.8)/\theta$, where k_{ap} is the apparent rate constant and $\theta = 2.303RT$ kcal mol⁻¹ (R is the ideal gas law constant, and T is absolute temperature). Inferences from the derived kinetic parameters suggest that initiation involves H-atom abstraction from either a vinyl or an aromatic fuel species.

Introduction

Autoxidation of aviation fuels is the origin of most surface-fouling problems in current aircraft.^{1,2} In addressing fuel-fouling problems, a primary goal is the determination of the kinetic parameters that describe hydrocarbon fuel autoxidation and control subsequent surface deposition. Autoxidation chemistry can be monitored from the initial O₂ depletion, the appearance of hydroperoxides, and the additional reaction products formed with more extensive conversion. Most studies have been based on reaction products in flask tests using paraffins^{3–9} or doped paraffins.^{10,11} With aviation fuels, product analysis is more complicated, but similar approaches have been made with the Shell flask rig.¹² Fodor and co-workers^{13–15} have completed detailed studies of hydroperoxide formation in jet fuels. Because

of difficulties in measuring dissolved O₂, kinetic investigations have been based on analysis of O₂ in the headspace.¹² Recent gas chromatography (GC) methodology has allowed fuel-oxidation measurements to be made *in situ* under nonisothermal¹⁶ and isothermal¹⁷ reaction conditions.

The near-isothermal flowing test rig (NIFTR) has been used to study the phenomenological kinetics for autoxidation and surface fouling of aviation fuels subjected to thermal stress.^{17,18} In NIFTR methodology fuel is subjected to thermal stressing in a single phase at fixed temperature, pressure, and initial O₂ concentration—conditions that are amenable to fundamental chemical studies. This technique involves a simple simulation of the extremely complicated conditions of temperature and fluid dynamics that exist in actual aircraft fuel lines.

Interpretation of NIFTR data is subject to complication if the autoxidation involves surface catalysis; this is certainly the case if virgin stainless steel tubing is used as the heat-exchanger surface. In contrast, the use of Silcosteel-passivated¹⁹ heat-exchanger tubing reduces the influence of surface catalysis and subsequent problems associated with interpretation of kinetic data. The significance of the present study is twofold. First, we determine the reaction order for O₂ loss for homogeneous autoxidation of Jet-A fuel (POSF-2827) using Silcosteel-passivated¹⁹ heat-exchanger tubing. Second, we determine the kinetic rate parameters for homogeneous autoxidation of POSF-2827 fuel that are not perturbed by surface catalysis. To the authors' knowl-

* Abstract published in *Advance ACS Abstracts*, July 15, 1996.

(1) Edwards, T.; Anderson, S. D.; Pearce, J. A.; Harrison, W. E., III. High Temperature Fuels—An Overview. AIAA Paper 92-0683, presented at the AIAA 30th Aerospace Sciences Meeting and Exhibit, Reno, NV, Jan 6–9, 1992.

(2) Edwards, T. USAF Supercritical Hydrocarbon Fuels Interests. AIAA Paper 93-0807, presented at the AIAA 31st Aerospace Sciences Meeting and Exhibit, Reno, NV, Jan 11–14, 1993.

(3) Boss, B. D.; Hazlett, R. N. *Can. J. Chem.* **1969**, *47*, 4175–4182.

(4) Korcek, S.; Chenier, J. H. B.; Howard, J. A.; Ingold, K. U. *Can. J. Chem.* **1972**, *50*, 2285–2297.

(5) Mill, T.; Mayo, F.; Richardson, H.; Irwin, K.; Allara, D. L. *J. Am. Chem. Soc.* **1972**, *94*, 6802–6811.

(6) Camacho Rubio, F.; Diaz Rodriguez, F.; Fernandez Gonzalez, F.; Moreno Himenez, V. *Anal. Quim.* **1979**, *76*, 261–264.

(7) Jensen, R. K.; Korcek, S.; Mahoney, L. R.; Zinbo, M. *J. Am. Chem. Soc.* **1979**, *101*, 7574–7584; **1981**, *103*, 1742–1749.

(8) Garcia-Ochoa, F.; Romero, A.; Querol, J. *Ind. Eng. Chem. Res. Dev.* **1989**, *28*, 43–48.

(9) Blaine, S.; Savage, P. E. *Ind. Eng. Chem. Res.* **1991**, *30*, 2185–2191.

(10) Reddy, K. T.; Cernansky, N. P.; Cohen, R. S. *Energy Fuels* **1988**, *2*, 205–213.

(11) Jones, E. G.; Balster, W. J. ASME Paper 92-GT-122, presented at the 37th ASME International Gas Turbine and Aeroengine Congress and Exposition, Cologne, Germany, June 1–4, 1992.

(12) Kendall, D. R.; Mills, J. S. *Ind. Eng. Chem. Prod. Res. Dev.* **1986**, *25*, 360–366.

(13) Fodor, G. E.; Naegeli, D. W.; Kohl, K. B. *Energy Fuels* **1988**, *2*, 729–734.

(14) Fodor, G. E.; Naegeli, D. W. *Prepr. Pap.—Am. Chem. Soc., Div. Fuel Chem.* **1990**, *35* (4), 1267–1276.

(15) Fodor, G. E.; Naegeli, D. W.; Turner, L. M. *Prepr.—Am. Chem. Soc., Div. Pet. Chem.* **1992**, *37* (2), 403.

(16) Heneghan, S. P.; Martel, C. R.; Williams, T. F.; Ballal, D. R. *J. Eng. Gas Turb. Power* **1993**, *115*, 480–484.

(17) Jones, E. G.; Balster, W. J. *Energy Fuels* **1993**, *7*, 968–977.

(18) Jones, E. G.; Balster, L. M.; Balster, W. J. *Energy Fuels* **1995**, *9*, 906–912.

(19) Silcosteel tubing, Restek Corporation, Bellefonte, PA.

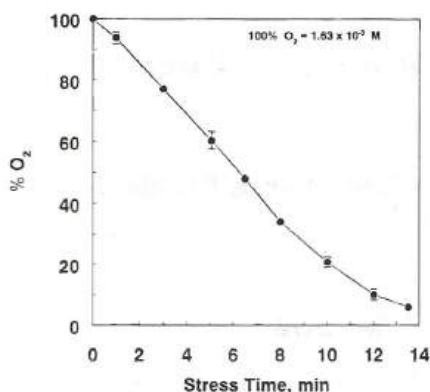


Figure 1. Repetitive NIFTR measurements for percent residual dissolved O_2 vs stress time at 458 K; 100% corresponds to fuel saturated with respect to air under ambient conditions. Error bars correspond to one standard deviation.

edge, this is the first report of an order analysis for jet fuel autoxidation free from the complications of surface catalysis. The kinetic data are discussed with reference to initiation mechanisms that may be inferred from the order dependence of the O_2 loss and the conventional chain mechanism expected for homogeneous autoxidation.

Experimental Section

POSF-2827 is a representative straight-run Jet-A fuel having a breakpoint temperature of 539 K as determined from the jet fuel thermal oxidation test (JFTOT), a total sulfur content of 0.079% (w/w), and a specific gravity of 0.8072. All experiments were conducted using the NIFTR that has been described in detail elsewhere.^{17,18} Reaction occurred during passage of fuel through 0.318-cm-o.d., 0.216-cm-i.d. passivated tubing clamped tightly within an 81.3-cm heated-Cu-block heat exchanger. Stress duration—or residence time within the heated tube—was varied by changing the fuel flow rate and was calculated from the plug flow. Relative dissolved O_2 concentrations of unstressed and stressed fuel were measured according to the GC method of Rubey.²⁰

Three types of NIFTR experiments were conducted. First, five identical repetitive measurements at 458 K were made on air-saturated fuel to assess the repeatability of the O_2 measurements for this fuel.

Second, a series of measurements was carried out at 458 K using different initial O_2 concentrations to assess the oxygen dependence of the reaction rate. These measurements were conducted with fuel having a dissolved O_2 content within the range 2.5–100% O_2 saturation under ambient conditions. Gas blending of O_2 and N_2 was achieved using a Porter CM 4 interface module and F200 thermal mass flow controllers. Fuel was then sparged with blended gas for 30 min at room temperature using a 25- μ m porosity glass plug. Oxygen- and air-saturated fuels contain 308 and 64.7 ppm of O_2 , respectively. The slope of a linear plot of the integrated GC intensity versus sparge blend was used to determine the response factor of the GC. The high correlation coefficient ($r^2 > 0.99$) of the data fit was indicative of the precision of the blending process. Dissolved O_2 signals measured in air-saturated and 21% O_2 blend-saturated fuel differed by <3%. Rates of oxygen depletion were determined from the slopes of the O_2 versus stress time plots in the initial stages of reaction.

In the third experimental series, O_2 depletion data were collected from 438 to 488 K using air-saturated fuel for the purpose of evaluating Arrhenius parameters. Rates of reaction

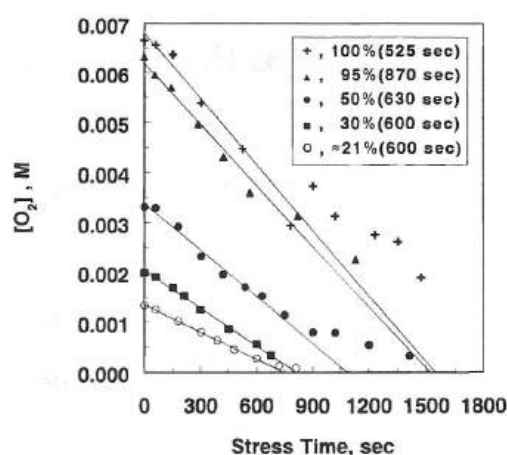


Figure 2. Variation of dissolved O_2 concentration (21–100%) with stress time at 458 K. Parenthetical entries are times used to calculate the initial rate.

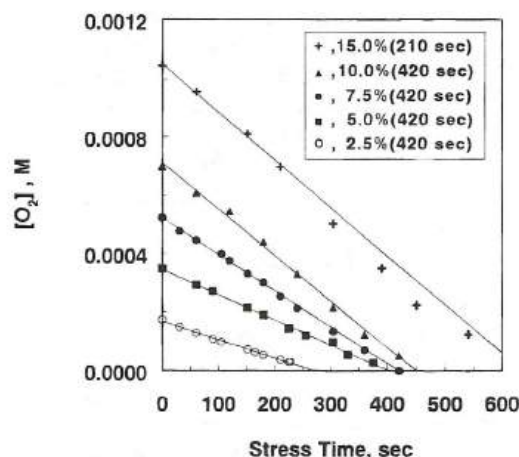


Figure 3. Variation of dissolved O_2 concentration (2.5–15%) with stress time at 458 K. Parenthetical entries are times used to calculate the initial rate.

were expressed as moles per liter-second ($M s^{-1}$) from the fuel densities in the range 438–488 K.

Results and Discussion

Data. A plot of the O_2 depletion for five repetitive experiments conducted at 458 K for air-saturated fuel is shown in Figure 1. The error bars correspond to one standard deviation. These data have an uncertainty on the order of $\pm 3\%$ from 0 to 100% of the O_2 depletion. O_2 depletion data for measurements made at 458 K for different initial relative O_2 concentrations ($[O_2]_0$) are shown in Figures 2 and 3. The tangents in Figures 2 and 3 represent the initial rates with $[O_2] = [O_2]_0$. The parenthetical entries in the figure boxes are the times used to compute the initial rates.

The rate of the reaction may be expressed empirically as

$$-d[O_2]/dt = k_{ap}[O_2]^n[RH]^m \quad (1)$$

where k_{ap} is an apparent rate constant, $[O_2]$ and $[RH]$ are oxygen and fuel concentrations, and n and m are reaction orders. In logarithmic coordinates, for a constant $[RH]$, eq 1 should be linear, having a slope equivalent to the reaction order n . An order plot based on this approach using tangents taken from Figures 2 and 3 is given in Figure 4; the slope of the line indicates

(20) Rubey, W. A.; Striebich, R. C.; Tissandier, M. D.; Tirey, D. A.; Anderson, S. D. *J. Chromatogr. Sci.* **1995**, *33*, 433–437.

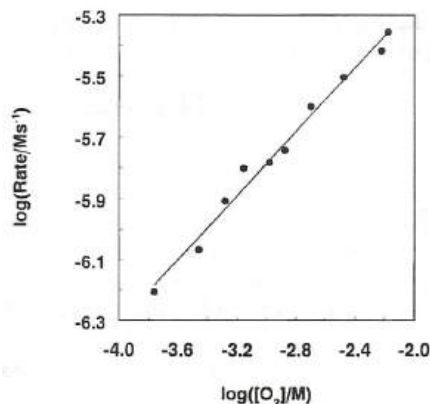
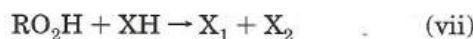
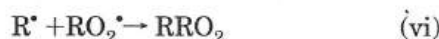
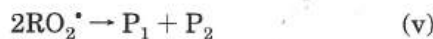
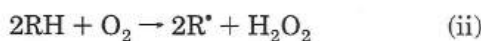
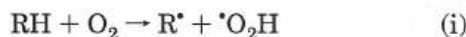


Figure 4. Order plot at 458 K for air-saturated POSF-2827 fuel.

that n is 0.52 ± 0.026 . Previous isothermal work by Jones and Balster has suggested a zero-order O_2 dependence;¹⁷ the nonisothermal studies of Ballal and co-workers have indicated either a first-order¹⁶ or a zero-order²¹ O_2 dependence.

Reaction Mechanism. Fuel oxidation may be approximated by the following reaction mechanism:



where R^* is a radical, RO_2^* is a peroxy radical, RO_2H is hydroperoxide, P_1 , P_2 , and RRO_2 are molecular species formed by termination, XH is a natural inhibitor or retarder, and X_1 and X_2 are molecular products from reaction of hydroperoxide with inhibitor. Reactions i and ii are two potential initiation pathways that have been previously proposed for hydrocarbon initiation,^{22a,23} consistent with the observed reaction order of 0.5 determined from the O_2 dependence. The initiation reaction would correspond to either reaction i or ii; reactions iii and iv are chain propagation, and reactions v and vi are potential termination reactions. Reaction v is the primary termination step since $[RO_2^*] > [R^*]$ and $k_{iii} \gg k_{iv}$ at steady state. It is proposed that most of the intermediate hydroperoxide is depleted by sulfur-containing compounds in POSF-2827, as suggested by reaction vii.

The plots in Figures 2 and 3 exhibit a slight curvature that may be indicative of autocatalysis; the degree of curvature is substantially less than observed in virgin

(21) Heneghan, S. P.; Martel, C. R.; Williams, T. F.; Ballal, D. R. *J. Eng. Gas Turbines Power* **1995**, *117*, 120–124.

(22) Benson, S. W. *Thermochemical Kinetics*; Wiley: New York, 1976; (a) p 239, (b) pp 148–149.

(23) Carlsson, D. J.; Robb, J. C. *Trans. Faraday Soc.* **1966**, *62*, 3403–3415.

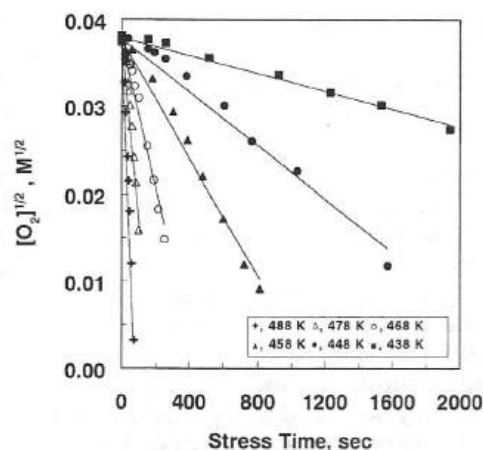


Figure 5. Rate-law plots for dissolved O_2 from 438 to 488 K.

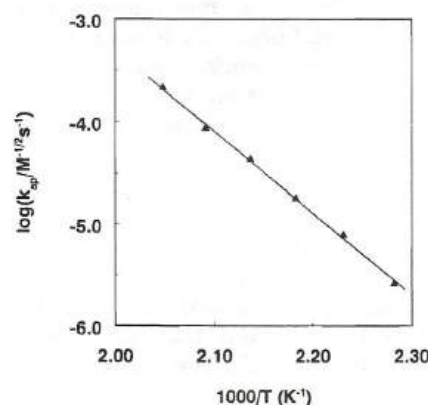


Figure 6. Arrhenius plot for POSF-2827 autoxidation over the range 438–488 K.

stainless-steel tubes.^{17,24} This suggests that the disappearance of RO_2H occurs predominantly by reaction vii and that any dissociation of RO_2H is negligible.

Consistent with the observed reaction order of $n = 0.5$ for O_2 and the assumption that $m = 1$, eq 1 may be rewritten as

$$-d[O_2]/dt = k_{ap}[O_2]^{1/2}[RH] \quad (2)$$

Integration of eq 2 leads to

$$[O_2]^{1/2} = [O_2]_0^{1/2} - (k_{ap}/2)[RH]t \quad (3)$$

where t is time. Equation 3 indicates a linear time dependence for $[O_2]^{1/2}$ depletion, with a slope equivalent to $k_{ap}[RH]/2$. Plots of the air-saturated data in the range 438–488 K according to eq 3 are shown in Figure 5; the solid lines are linear least-squares fits. The rate constants, k_{ap} , were calculated from the slopes of the lines in Figure 5, under the assumption that $[RH] \approx [RH]_0$ (fuel molarity was derived from the fuel density at each temperature and the assumption of an average hydrocarbon chain length of 13). An Arrhenius plot for these data is given in Figure 6. Statistical analysis of the data led to

$$\log(k_{ap}/M^{-1/2}s^{-1}) = (12.9 \pm 0.4) - [(36.9 \pm 0.8)/\theta] \quad (4)$$

where the errors correspond to one standard deviation and $\theta = 2.303RT$ kcal mol⁻¹ (R is the ideal gas law

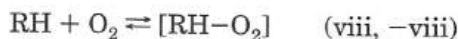
(24) Jones, E. G.; Balster, W. J.; Vonada, M. R.; Pickard, J. M. *Prepr.-Am. Chem. Soc., Div. Pet. Chem.* **1994**, *39* (1), 10–13.

constant, and T is absolute temperature). The apparent activation energy ($E = 36.9 \pm 0.8$ kcal mol⁻¹) summarized in eq 4 is consistent with the values previously reported: 35.5 and 30.5 kcal mol⁻¹ by Ballal and co-workers^{16,21} and 35.8 kcal mol⁻¹ by Jones and Balster.¹⁷

Discussion. The reproducibility of the observed O₂ loss data obtained from the repetitive measurements and the absence of any pronounced S-shaped dependence are indications that the passivated heat-exchanger tubing is effective in eliminating most, if not all, of the autocatalysis observed previously when POSF-2827 was subjected to thermal stress in contact with virgin stainless steel. Therefore, considerable confidence may be placed in the reaction order obtained for O₂ and the apparent kinetic parameters summarized in eq 4.

The potential initiation mechanisms that may be inferred from the half-order O₂ dependence will now be addressed. In previous work using 2,2'-azobis[2-methylpropionitrile] (AIBN) as an initiator over the temperature range 393–413 K, we determined $\log(k_p/(2k_t)^{1/2})/M^{-1/2} \text{ s}^{-1/2} = (7.08 \pm 0.27) - (18.6 \pm 0.5)/\theta$, where k_p and $2k_t$ are rate constants for propagation and termination, respectively.²⁴ For these data it was determined independently that the spontaneous surface-catalyzed oxidation of POSF-2827 fuel was negligible within this low experimental temperature range. Thus, rate parameters determined from the AIBN data may be combined with eq 4 to infer the A factor for initiation.

Two initiation mechanisms consistent with our observed O₂ dependence are reactions i and ii. Reaction i would be expected to have an activation energy approximately equal to the endothermicity^{22a} of 31 kcal mol⁻¹. The mechanism for reaction ii, as proposed for hydrocarbons by Carlsson and Robb,²³ may be expressed as



where $[\text{RH}-\text{O}_2]$ is a complex between O₂ and the substrate responsible for initiation.

The usual steady-state relation for oxidation involving a second-order termination mechanism may be expressed as

$$-d[\text{O}_2]/dt = k_p(R_i/2k_t)^{1/2}[\text{RH}] \quad (5)$$

Comparison of eqs 2 and 5 with $R_i = k_i[\text{O}_2][\text{RH}]$ for reaction i leads to

$$k_{\text{ap}} = k_p(k_i/2k_t)^{1/2}[\text{RH}]^{1/2} \quad (6)$$

In similar fashion for reaction ii, where $R_i = k_{\text{ix}}K[\text{RH}]^2[\text{O}_2]$, comparison of eqs 2 and 5 leads to

$$k_{\text{ap}} = k_p(k_{\text{ix}}K/2k_t)^{1/2}[\text{RH}] \quad (7)$$

where $K = k_{\text{viii}}/k_{-\text{viii}}$. At the mean temperature of 458 K, with $\log[k_p/(2k_t)^{1/2}/M^{-1/2} \text{ s}^{-1/2}] = (7.08 \pm 0.27) - (18.6 \pm 0.5)/\theta$, $[\text{RH}] = 3.75$ and with recognition that $\log k_{\text{ap}} = \log A_{\text{ap}} - E_{\text{ap}}/\theta$, eq 6 implies that $\log(A_i/M^{-1} \text{ s}^{-1}) = 11.2 \pm 0.5$. The calculated A_i is in good agreement with that expected for a bimolecular abstraction reaction^{22a} with $\log(A/M^{-1} \text{ s}^{-1}) = 11.0$. In contrast, for the termolecular process in which initiation involves H-atom abstraction from the complex $[\text{RH}-\text{O}_2]$, eq 7 leads to $\log[A_{\text{ix}}(A_{\text{viii}}/A_{-\text{viii}})/M^{-2} \text{ s}^{-1}] = 10.6 \pm 0.5$. The assumption^{22b} that $\Delta S_{\text{viii}} \geq -17$ cal mol⁻¹ K⁻¹ may be combined with $A_{\text{viii}}/A_{-\text{viii}} = 10^{\Delta S/(2.303R)}$ (ΔS is the entropy change for the standard state in molar concentration units) to infer $A_{\text{viii}}/A_{-\text{viii}} = 10^{-3.7} \text{ M}^{-1}$. Therefore, from eq 7, one expects $\log(A_{\text{ix}}/M^{-1} \text{ s}^{-1}) \approx 14.3$. The magnitude of A_{ix} is consistent with the point that reaction ix would proceed with an appreciable increase in entropy. The similarity in magnitude of $\log(A_i/M^{-1} \text{ s}^{-1}) = 11.2 \pm 0.5$ and $\log[A_{\text{ix}}(A_{\text{viii}}/A_{-\text{viii}})/M^{-2} \text{ s}^{-1}] = 10.6 \pm 0.5$ indicates that distinctions between mechanisms may not be possible from a simple structural analysis of the A factors.

However, from eq 5 the apparent activation energy (E_{ap}) for autoxidation involving H-atom abstraction initiation (reaction i) may be expressed as

$$E_{\text{ap}} = E_p + [(E_i - E_t)/2] \quad (8)$$

Similarly, for the termolecular process, E_{ap} may be expressed as

$$\begin{aligned} E_{\text{ap}} &= E_p + [(E_{\text{ix}} - E_t + \Delta H_{\text{viii},-\text{viii}})/2] \\ &= E_p + [(E_{\text{ix}} - E_t)/2] \quad \text{if } \Delta H_{\text{viii},-\text{viii}} \approx 0 \end{aligned} \quad (9)$$

Equations 8 and 9 are identical if it is assumed that $\Delta H_{\text{viii},-\text{viii}}$ is zero and that $k_{\text{ix}} = k_i$. The AIBN data,²⁴ $E_p - E_t/2 = 18.6 \pm 0.5$ kcal mol⁻¹, may be combined with $E_{\text{ap}} = 36.9 \pm 0.8$ kcal mol⁻¹ from eq 4 to infer $E_i = 36.6 \pm 0.9$ kcal mol⁻¹—this value is reasonably near the value^{22a} of 31 kcal mol⁻¹ expected for an H-atom abstraction reaction. Therefore, with a view toward simplicity, one would favor reaction i as the preferred mode of initiation.

Acknowledgment. This work was sponsored by Wright Laboratory, Aero Propulsion and Power Directorate, Wright-Patterson Air Force Base, OH, under USAF Contract F33615-95-C-2507. We thank Ms. Lori Balster for performing the dissolved O₂ measurements and Ms. Marian Whitaker for lending editorial assistance.

EF9600319